International Journal of Heat and Fluid Flow 69 (2018) 73–82

Contents lists available at ScienceDirect

International Journal of Heat and Fluid Flow

journal homepage: www.elsevier.com/locate/ijhff

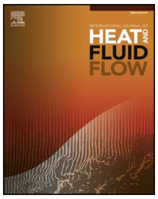

Wavelet multi-scale analysis of the circular cylinder wake under synthetic jets control

Li-Hao Feng[a,*], Ling-Ke Ran[a,b]

[a] Fluid Mechanics Key Laboratory of Education Ministry, Beijing University of Aeronautics and Astronautics, Beijing 100191, China
[b] Wuhan Second Ship Design and Research Institute, Wuhan 430064, China

ARTICLE INFO

Keywords:
Wavelet multi-scale analysis
Circular cylinder
Synthetic jet

ABSTRACT

The wavelet method is used to study the multi-scale vortical structures of the flow around a circular cylinder without and with synthetic jet control at $Re = 950$. The velocity field is decomposed into 9 wavelet components, including one approximation component and 8 detail components. The first component shows the flow characteristics at low frequency. The dominant components represent large-scale vortical structures in the flow and they show similar distributions for the same wake pattern. Other detail components reflect the characteristics of relatively small-scale structures. The individual vortex dynamics underlying the complex flow can be extracted and thus reconstructed by the approximation and dominant components. Thus, we show an effective approach to reveal the flow physics from the complex flow.

1. Introduction

As a typical bluff body, the flow around a circular cylinder and its control is of great concern due to both academic values and potential applications in engineering. In the past, many passive and active methods were introduced to control the vortex shedding behind bluff bodies, such as geometric modification, splitter plate, base bleed, oscillation, and rotary (Choi et al., 2008). In recent decades, novel active flow control techniques, such as plasma actuators (Wang et al., 2013) and synthetic jets (Glezer and Amitay, 2002; Jabbal and Zhong, 2010), have been studied and applied widely. The synthetic jet is formed by the periodic ejection and suction of fluids from an orifice (Smith and Glezer, 1998). The synthetic jets have been applied in various fields (Zhang et al., 2008), and one of the fields is to control the flow around a circular cylinder. It has been found that the synthetic jets could delay flow separation (Béra et al., 2000; Tensi et al., 2002), reduce cylinder drag (Fujisawa and Takeda, 2003; Naim et al., 2007), and change wake patterns (Feng and Wang, 2010; Feng et al., 2011).

The flow around a circular cylinder and its control involve different complex flow phenomena, such as flow separation, shear layer instability, and vortex dynamics. Thus, it is usually difficult to directly extract the useful information from the experimental or numerical data. To solve this problem, several data processing methods have been proposed to simplify the study of complex flow and better understand the flow physics. These methods include velocity decomposition (Kim et al., 2006; Feng and Wang, 2010), proper orthogonal decomposition (POD) (Konstantinidis et al., 2007; Feng et al., 2011; Liu et al., 2011; Zhang et al., 2014), and dynamic mode decomposition (DMD) (Pan et al., 2011; Bagheri, 2013; Chen et al., 2012; He et al., 2013; Zhang et al., 2014; Liu and Zhang 2015). The velocity decomposition separates a velocity signal into the mean component, the periodic mean component which reflects contributions of the large-scale organized coherent structures, and the random component which reflects contributions of the small-scale turbulent structures. Both the POD and DMD can reduce the dimensionality of the original data by decomposing the global flow field into different modes, which are based on the occupied energy and the characteristic frequency, respectively. The large-scale coherent structures usually occupy most of the energy and may dominate the global evolution of the flow field, thus their features can be well described based on the mode decomposition.

The above methods have the individual advantages. However, the flow structures extracted by these methods were mainly about the coherent structures in the previous studies, while the structures other than the coherent ones were of little concern. On the other hand, the wavelet method can distill the multi-scale coherent structures from the original flow fields (Daubechies, 2012). The main idea of multi-resolution analysis is decomposing a signal into a series of components, which have different frequency bandwidths or different time scales. The properties of the signal with different temporal-and-spatial scales can be obtained by analyzing these decomposed components. It has also been proved as a powerful tool to analyze different kinds of flow, such as turbulence (Meneveau, 1991; Jiang and Zhang, 2005), pipe flow

---

[*] Corresponding author.
E-mail address: lhfeng@buaa.edu.cn (L.-H. Feng).

https://doi.org/10.1016/j.ijheatfluidflow.2017.12.003
Received 5 April 2017; Received in revised form 14 November 2017; Accepted 3 December 2017
0142-727X/

(Vétel et al., 2010), jet (Grizzi and Camussi, 2012; Watanabe et al., 2014), and flow around a step (Lee and Sung, 2001; Schram et al., 2004), a mirror (Rinoshika and Watanabe, 2010), and bluff bodies (Rinoshika and Omori, 2011). There are also a number of studies about the wavelet analysis of flow around a circular cylinder (Hangan et al., 2001; Rinoshika and Zhou, 2005a, b; Zhou et al., 2006; Razali et al., 2010; Indrusiak and Möller, 2011). In particular, Rinoshika and his colleagues have done a series of pioneering works based on hot-wire and particle image velocimetry (PIV) measurements, where the vortical structures at different wavelet components were studied.

In this study, the wavelet method is used to study the flow around a circular cylinder without and with synthetic jet control. For the controlled cylinder wake, there exist multi-scale vortical structures that might be related to the natural frequency, the excitation frequency, their harmonics or non-harmonics. It is difficult to directly analyze such flow by using conventional methods. Thus, with the help of the wavelet method, the main concern here is to extract the multi-scale vortical structures from the flow field, with a view to reveal the flow physics of cylinder wake under external excitations.

2. Experimental set-up and method

The experiment was conducted in a low-speed water tunnel at the Beijing University of Aeronautics and Astronautics. The water tunnel has a test section with size 0.6 m × 0.6 m × 4.8 m. The free-stream velocity could be continuously changed lower than 200 mm/s and the streamwise turbulent intensity was no more than 0.8%. The experimental circular cylinder had an outer diameter of $D = 30$ mm, an inner diameter of $d = 22$ mm, and a length of $l = 500$ mm, as shown in Fig. 1. The cylinder was horizontally mounted across the test section of the water tunnel. During the experiments, the free-stream velocity was fixed at 41.8 mm/s, corresponding to the Reynolds number $Re = 950$. The natural frequency for the Karman vortex around the cylinder was detected to be $f_0 = 0.29$ Hz here, corresponding to the Strouhal number $St = 0.21$, which agrees well with the literature data from Zdravkovich (1997).

A 1 mm width narrow slot with length of 50 mm as the exit of the synthetic jet was disposed onto the external surface in the mid-span region of the experimental cylinder, as shown in Fig. 1. It was connected to the horizontal section of an "L"-shape hollow circular cylinder. A piston controlled by a servo electromotor was inside the vertical section of the "L"-shape cylinder that was fixed onto the sidewall of the test section. The circular motion performed by the servo electromotor could be converted into the reciprocating motion of the piston by a centre-setting crank mechanism. Thus, the fluids could be ejected and sucked from the narrow slot periodically, and thus forming the synthetic jet vortex pair. The control parameters for the synthetic jet system were the excitation amplitude of the piston and the excitation frequency for vortex generation. For the present control cases, the excitation amplitude was fixed at $A = 5.5$ mm, while the excitation frequency was set at $f_e = 0.50$ Hz and 1.00 Hz, corresponding to the synthetic jet Reynolds number $Re_{\bar{U}0} = 38$ and 76, respectively. Here, the Reynolds number $Re_{\bar{U}_0}$ was based on the time-averaged blowing velocity $\bar{U}_0$ of the synthetic jet during one period. The excitation frequencies equal to harmonics of the natural frequency were not particular selected since the strength of the synthetic jet which is determined by the Reynolds number $Re_{\bar{U}_0}$ plays an more important role on the present control approach. More details of the experimental setup can be found in related studies (Feng and Wang, 2010; Feng et al., 2011).

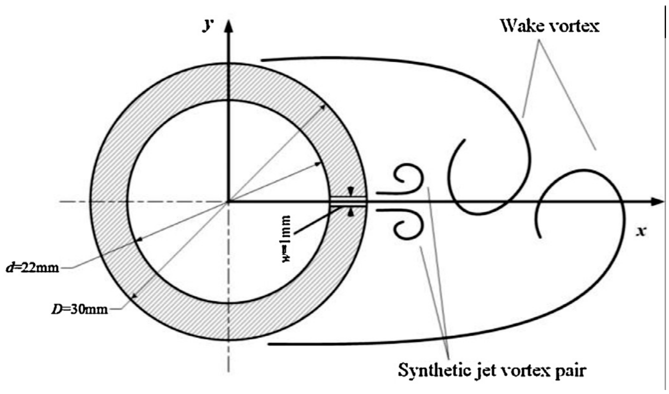

Fig. 1. Schematic of the experimental circular cylinder.

The time-resolved PIV was used to measure the two-dimensional flow field around the circular cylinder in the middle span. The measured flow field was illuminated by a continuous laser. The hollow glass beads with average diameter 5 μm and density 1.05 g/cm^3 were used as tracer particles. The field of view was captured by a CCD camera at a frequency of 100 Hz. The images had a spatial resolution of 640 × 480 pixels, corresponding to about 3D × 2D for the actual scales. A total of 8192 frames were used for the wavelet analysis for each case. The sizes of the interrogation window were set to 16 × 16 pixels, with 50% overlap in both streamwise and vertical directions. The cross-correlation algorithm with multi-grid iteration and window deformation was used to calculate the velocity flow field. The uncertainty of the measured velocity was less than 2 mm/s (Feng and Wang, 2010).

3. Wavelet decomposition technique

Orthogonal wavelet transform can be processed by multiplying the original data matrix with an orthogonal wavelet basis matrix, which is constructed with the wavelet filter coefficients (Rinoshika and Watanabe, 2010; Daubechies, 2012). The wavelet basis matrix contains two parts, namely the high-pass filter and the low-pass filter. When the data matrix multiplies the high-pass and low-pass filters, the approximation and detail coefficients can be obtained. Furthermore, the approximation coefficient can also be treated as a data matrix, which can be further transformed into two new coefficients. When this procedure is processed several times, a series of wavelet coefficients are obtained. These coefficients are orthogonal with each other and contain the information of the original data matrix in different frequency bands. On the other hand, when the wavelet coefficients multiply mirror filters, one can obtain several new data matrixes with different frequency bands that have physical meanings. A more detail procedure is described as follows.

For one-dimensional data matrix $\boldsymbol{V}^{\boldsymbol{N}} = [v_0, v_1, v_2, \ldots, v_{2N-1}]$, orthogonal wavelet transform is firstly processed in $2^{\boldsymbol{J}+\boldsymbol{M}}$ time resolution, where $\boldsymbol{J}$ is the maximum level which the data matrix can be decomposed, and $\boldsymbol{M} = \boldsymbol{N}–\boldsymbol{J} - \boldsymbol{1}$, is the minimum time resolution of the decomposed data. The approximation coefficient $\boldsymbol{C}_A^J$ and the detail coefficient $\boldsymbol{C}_D^J$ are obtained by multiplying data matrix $\boldsymbol{V}^{\boldsymbol{N}}$ with low-pass filter $\boldsymbol{F}_L^J$ and high-pass filter $\boldsymbol{F}_H^J$, respectively.

$$\begin{aligned} \boldsymbol{C_A}^{\boldsymbol{J}} &= \boldsymbol{V}^{\boldsymbol{N}} \times \boldsymbol{F_L}^{\boldsymbol{J}}, \\ \boldsymbol{C_D}^{\boldsymbol{J}} &= \boldsymbol{V}^{\boldsymbol{N}} \times \boldsymbol{F_H}^{\boldsymbol{J}}. \end{aligned} \tag{1}$$

Two new data matrixes $\boldsymbol{V}_A^J$ and $\boldsymbol{V}_D^J$, which are approximation component and detail component of the original data matrix, are obtained by multiplying the wavelet coefficients $\boldsymbol{C}_A^J$ and $\boldsymbol{C}_D^J$ with the mirror filters $\dot{\boldsymbol{F}}_L^J$ and $\dot{\boldsymbol{F}}_H^J$,

$$\begin{aligned} \boldsymbol{V}^{\boldsymbol{N}} &= \boldsymbol{V_A}^{\boldsymbol{J}} + \boldsymbol{V_D}^{\boldsymbol{J}}, \\ \boldsymbol{V_A}^{\boldsymbol{J}} &= \dot{\boldsymbol{F}}_{\boldsymbol{L}}{}^{\boldsymbol{J}} \times \boldsymbol{C_A}^{\boldsymbol{J}}, \\ \boldsymbol{V_D}^{\boldsymbol{J}} &= \dot{\boldsymbol{F}}_{\boldsymbol{H}}{}^{\boldsymbol{J}} \times \boldsymbol{C_D}^{\boldsymbol{J}}. \end{aligned} \tag{2}$$

The approximation component $\boldsymbol{V}_A^J$ contains the information of the low-frequency bandwidth of original data, and $\boldsymbol{V}_D^J$ contains high-frequency bandwidth information.

The next step is to decompose the approximation coefficient $\boldsymbol{C}_A^J$ into two coefficients $\boldsymbol{C}_A^{J-1}$ and $\boldsymbol{C}_D^{J-1}$ by multiplying it with filters $\boldsymbol{F}_L^{J-1}$ and